Aleksandar Jemcov
Associate Research Professor
Department of Aerospace and Mechanical Engineering, University of Notre Dame
USA

Joseph P. Gonzales
Graduate Student
Department of Aerospace and Mechanical Engineering, University of Notre Dame
USA

Joseph P. Maruszewski
ANSYS Fellow
ANSYS Inc., Evanston, IL
USA

Ryan T. Kelly
Senior Research Scientist
Notre Dame Turbomachinery Laboratory
Ignition Park, South Bend, IN
USA

Non-Iterative Wall Model Formula for Non-Equilibrium Boundary Layer Flows

A novel non-iterative (explicit) formulation of generalized wall functions that applies to equilibrium and non-equilibrium boundary layer flows was proposed. The proposed formulation uses a set of variables that are more useful for computational fluid dynamics codes as they allow for calculating wall shear stress without an iterative procedure. In addition, an explicit form of the formulation was provided that applies to wall models with and without pressure gradients. The new variable transformation casts the generalizedwall function into a new form that simplifies the implementation and evaluation of wall-shear stress in computational codes.

Keywords: *wall model, near-wall variables; turbulent boundary layer; wall-shear stress; variable transformation.*

1. INTRODUCTION

Time-averaged turbulence models based on Reynolds decomposition have been successfully used in simulations of practical engineering flows[1-5]. Some often used turbulence models include k-epsilon [6], k-omega [7], Spalart-Allmaras [8,9], v2f [10], to mention a few. The computational expense of time-averaged-based turbulence models in practical applications is primarily driven by the computational cost of resolving sharp gradients in the flow field near solid walls.The turbulent flows can be simulated without recourse to any turbulence models using the so-called Direct Numerical Simulation (DNS) of Navier-Stokes equations. However, the computational cost associated with DNS is prohibitively high [11,12] due to significant mesh resolution requirements near solid walls. Turbulence models based on Reynolds averaged Navier-Stokes (RANS) equations and corresponding turbulence models decrease the computational cost significantly. Even though the mesh resolution requirements are considerably lower than DNS, RANS models are still required to resolve the boundary layer to compute the correct wall shear stress τ_w and resolve the sharp velocity gradients in the vicinity of walls. Therefore, the wall treatment in RANS simulations remains one of the central questions in turbulent flow simulations.

The wall treatments in RANS simulations are broadly divided into two categories, namely wall-integrated and wall-modeled. Wall-integrated RANS models are typically called Low Reynolds Number (LRN) models and are capable of resolving the flowfield in all regions, including the boundary layer portion of the domain. In other words, LRN models can take into account the change of the local Reynolds number signifying the local ratio of inertial to viscous forces without any need for the special wall treatment. Other examples of LRN models are Spalart-Allmaras and k-omega SST models. However, LRN models require increased mesh resolution near the wall to accurately capture velocity gradients and compute the wall-shear stress.

On the other hand, wall-modeled RANS models cannot accurately represent the boundary layer flows, requiring a special set of boundary conditions called wall functions. The wall function provides a reduced-order model of the boundary layer's momentum equation, enabling accurate computation of the wall-shear stress. Wall functions are traditionally based on the velocity profile in the boundary layer, called the law of the wall, obtained by simplifying the time-averaged momentum equation in the streamwise direction.The simplified momentum equation is then integrated analytically to get the solution's closed-form [13, 14].

The first attempts to obtain the law of the wall date back to Prandtl [15,16], who obtained the velocity profile by introducing assumptions that the inertial and viscous forces were equally important in the laminar sublayer. In reality, inertial forces dominate the boundary layer's logarithmic (inertial) region [13]. Furthermore, the closed-form obtained by Prandtl did not take into account non-equilibrium effects due to pressure gradients and separated flows. In addition, Prandtl's law of the wall did not provide the velocity profile for the buffer region of the boundary layer. Several expressions of the law of the wall were developed to account for the presence of the buffer layer[17-20] by incorporating various assumptions and experimental observations. However, none of the proposed laws incorporated non-equilibrium effects. Hanjalic and Popovac [21] proposed the inclusion of the pressure gradient in the law of the wall.

Similarly, Röber [22] proposed a single expression for the velocity profile that included the effects of pressure gradients. Finally, Shih et al. [23] proposed a generalized form of wall functions applicable to a wide range of non-equilibrium flows. Other wall treatments include the two-layer approach [24] and non-equili–brium wall functions [25].

Received: February 2022, Accepted: March 2022
Correspondence to: Aleksandar Jemcov, Associate Research Professor, Department of Aerospace and Mechanical Engineering, University of Notre Dame, USA, E-mail: ajemcov@nd.edu
doi:10.5937/fme2201223J

One of the main difficulties in implementing wall functions is their implicit nature. For example, compu–tational codes require wall-shear stress to be computed to obtain the correct turbulent viscosity near the wall. However, the wall of the law gives the expression for velocity profile in the boundary layer. Therefore, the wall shear stress must be computed from the velocity profile, which is done through an iterative procedure. The need for the iterative procedure is discussed in the next section.

Given the difficulties with the existing expressions for the wall functions, the desired wall function should have the following characteristic:

1) Applicability to equilibrium and non-equilibrium boundary layer flows
2) Ability to evaluate wall-shear stress without recourse to iterative procedures

The wall function formulation that has the stated desired properties was proposed in this work. The formulation is based on a generalized wall function expression [23], which was transformed into a new set of variables to evaluate wall-shear stress explicitly.

2. WALL FUNCTION THEORY

The following expression gives the governing equations for incompressible turbulent fluid flow

$$\frac{\partial\left(\rho u_i\right)}{\partial t}+\frac{\partial\left(\rho u_i u_j\right)}{\partial x_i}=-\frac{\partial p}{\partial x_i}+\frac{\partial \sigma_{ij}}{\partial x_i} \tag{1}$$

$$\partial_i u_i = 0 \tag{2}$$

Cartesian tensor notation was used in Equations 1 and 2, where indexes i and j take the values denoting three directions labeled (x,y,z). All quantities in Equa–tions 1 and 2 are time-averaged quantities. The Boussi–nesq assumption was used to represent the stress tensor σ_{ij}

$$\sigma_{ij}=\left(\mu+\mu_t\right)2S_{ij} \tag{3}$$

$$S_{ij}=\frac{1}{2}\left(\frac{\partial u_i}{\partial x_i}+\frac{\partial u_j}{\partial x_i}\right) \tag{4}$$

Here the symbol μ is molecular, whereas μ_t is turbulent viscosity. Equation 1 is a time-averaged, constant density form of momentum equation applicable to incompressible turbulent flows. No special notation was used to denote time-averaged quantities.

Equation 1 is simplified in the boundary layer, assuming that the pressure is uniform in the wall-normal direction throughout the boundary layer. Moreover, the flow is considered to be essentially one dimensional and pressure gradient-free in a streamwise direction denoted by the symbol x, yielding the following non-dimen–sional expression [13, 23]:

$$\left(1+v_t^+\right)\frac{du^+}{dy_t^+}=1, v_t^+=\frac{v_t}{v} \tag{5}$$

Symbols appearing in Equation 1 are defined as follows

$$u^+=A\left(y_t^+\right)^B, A=8.3, B=\frac{1}{7}, y_t^+>11.81 \tag{6}$$

where u is a time-averaged velocity in the streamwise direction, y is the distance in the wall-normal direction, and v is molecular kinematic viscosity. The non-dimensional quantities u^+ and y_t^+ are the non-dimensi–onal velocity and wall distance. The friction velocity is defined as

$$u_t=\sqrt{|\tau_w|/\rho} \tag{7}$$

Equation 3 provides the relationship between wall shear stress, friction velocity, and density. Therefore, Equation 5 must be solved to obtain the wall-shear stress.

2.1 Zero-pressure gradient wall functions

Strictly speaking, Equation 5 describes one-dimensional flows without a pressure gradient. For example, the flat plate boundary layer without the pressure gradient is a prototypical flow approximated by Equation 1. Prandtl [15] provided the analytical solution for the velocity profile over the flat plate with zero pressure gradient by integrating Equation 1 to obtain the following expression:

$$\frac{u}{u_t}=\frac{1}{\kappa}\ln\left(\frac{u_t y}{v}\right)+B \tag{8}$$

$$u^+=\frac{1}{\kappa}\ln\left(y_t^+\right)+B, y_t^+>10.8, \kappa=0.41, B=5.0$$

The first part of Equation 8 was obtained by inte–grating Equation 5,assumingthe turbulent viscosity is negligible in the laminar sublayer. Therefore, in the laminar sublayer, inertial and viscous forces due to molecular diffusion are of the same order allowing turbulent viscosity to be neglected. On the other hand, the second part of Equation 8 is obtained by integrating in the wall-normal direction from the wall to infinity. The resulting profile is called the logarithmic profile. Prandtl's law of the wall ignores the buffer region, and the two solutions are matched for the value $y_t^+ = 10.8$ to give a law applicable for all non-dimensional wall distance values.

A closer inspection of Equation 8 reveals that for any values of non-dimensional wall distance greater than 10.8, it is necessary to employ an iterative proce–dure. The need for iteration becomes apparent when the definition of non-dimensional velocity is examined. Equation 6 indicates that to solve Equation 5, the value of non-dimensional wall distance must be known, which depends on non-dimensional velocity. When Equation 6 is substituted into Equation 7, the following expression is obtained:

$$\frac{u}{u_t}=\frac{1}{\kappa}\ln\left(\frac{u_t y}{v}\right)+B \tag{9}$$

Equation 9 defines a non-linear function that re–quires an iterative procedure to determine the friction

velocity. Equation 5 is used to solve the friction velocity using an iterative procedure. The corresponding turbulent viscosity is computed once the friction velocity is known, thus allowing the momentum and turbulence model equations to be solved. However, in finite volume codes, the iterative procedure is repeated for each face on the wall boundary resulting in the complex implementation of wall functions and incre–ased computational expense.

Prandtl's law of the wall is an example of an implicitly defined wall function. Even a deceptively simple expression of Equation 5 requires an iterative procedure to compute the friction velocity and the wall-shear stress. Prandtl's law of the wall is not commonly used in the definition of wall functions as it ignores the buffer zone. Ignoring the buffer layer leads to inaccurate results of wall-shear stress in situations when the non-dimensional wall distance falls within the range of the buffer zone. Moreover, Prandtl's law of the wall was de–rived under the assumption of the zero pressure gradient. Most practical flows will have pressure gra–dient gra–dients in the near-wall region rendering the wall function based on Prandtl's law inaccurate or completely wrong.

In an attempt to define a continuous expression for the law of the wall with zero pressure gradient that takes into account the buffer zone, Spalding [17] proposed the following form of the law of the wall:

$$y_t^+ = u^+ + 0.1108\left[e^{4u^+} - 1 - 0.4u^+ - \frac{\left(0.4u^+\right)^2}{2!} - \frac{\left(0.4u^+\right)^3}{3!} - \frac{\left(0.4u^+\right)^4}{4!}\right] \tag{10}$$

While Spalding's proposal is an improvement over Prandtl's law of the wall, an iterative procedure is required to evaluate the friction velocity. The iterative procedure typically employed to compute the friction velocity from Equation 10 is Newton iterations.A quadratic convergence characterizes Newton iterations if a suitable initial condition is used to start the iterations. Due to its quadratic convergence, Newton iterations converge within several iterations. However, if the initial value of the iterations was not within the radius of convergence, Newton iterations diverge very quickly. The divergence of the iterative procedure may lead to incorrect values of friction velocity and consequently to errors in turbulent viscosity near the wall. The divergence in Newton iterations does not necessarily lead to the overall divergence of the CFD simulation. Instead, the iterations may produce erroneous values that are hard to detect and correct.

Given that the Newton linearization of Equation 10must be implemented in computational codes, it is safe to state that code complexity may be significant. In addition, the Newton iterations must be done for each face of a finite volume on the boundary leading to increased computational cost. Finally, Spalding's wall function does not include pressure gradient, thus leading to significant errors for non-equilibrium boundary layer flows.

Pieringer and Sanz [25] sought to improve upon Spalding's wall function by incorporating the shear-stress distribution perpendicular to the wall surface, mainly determined by pressure gradients. However, their model still requires an iterative approach to cal–culate shear stress.

Spalding's proposed form of the law of the wall resulted in a non-linear function that contained expo–nential terms. To simplify the law of the wall while providing a unified expression valid in all regions of the boundary layer, Musker [18] proposed the following function:

$$\frac{1}{v_t^+} = \frac{1}{c\left(y_t^+\right)^3} + \frac{1}{\kappa y_t^+},\ C = 0.001093, \kappa + 0.41 \tag{11}$$

The simplifaction proposed by Musker was based on the inverse weighting of two different functions. The first function represented the inertial region of the bou–ndary layer given by the following expression

$$f_1\left(y_t^+\right) = C\left(y_t^+\right)^3 \tag{12}$$

While the first function was suitable for the laminar sublayer

$$f_2\left(y_t^+\right) = \kappa y_t^+ \tag{13}$$

The inverse function weighting of the buffer zone was postulated to be well approximated. The smooth transition is obtained between two regions, namely the laminar sublayer and the inertial layer.

Musker's law of the wall provides the correct scaling of the turbulent viscosity close to the wall in the wall-normal direction, namely $v_t^+ \sim \left(y_t^+\right)^3$. The proposed turbulent viscosity function was used together with Reynolds averaged momentum equations to produce the dimensionless velocity gradient given by the expression

$$\frac{du^+}{dy_t^+} = \frac{\kappa + C\left(y_t^+\right)^2}{\kappa + C\left(y_t^+\right)^2 + C\left(y_t^+\right)^3} \tag{14}$$

Equation 14 was integrated to yield the law of the wall as follows:

$$u^+ + 5.424\tan^{-1}\left(\frac{2y_t^+ - 8.15}{16.7}\right) + \ln\left(\frac{\left(y_t^+ - 10.6\right)^{4.6}}{\left(y_t^{+2} - 8.15y_t^+ + 86.0\right)^2}\right) - 3.52 \tag{15}$$

Despite the simplifying assumptions used in the derivation of Equation 15, an iterative procedure is still needed to compute the friction velocity. Therefore, the Newton iterations may diverge similarly as in the case of Spalding's law of the wall. Furthermore, Musker's law of the wall did not include pressure gradients, and it is not suitable for non-equilibrium boundary layer flows.

The law of the wall proposed by Werner and Wengle [19, 26] provided an explicit formula for computing the non-dimensional velocity as follows

$$r^+ = u^+ y_t^+ \tag{16}$$

$$p^+ = \frac{v}{\rho u_t^3}\frac{dp}{dx} \tag{17}$$

The proposed formula was based on the piece-wise expression that is valid for all values of y_t^+. Moreover, Werner and Wengles's law of the wall yields the following expression for the wall-shear stress:

$$\frac{|\tau_w|}{\rho} = v\frac{|u|}{y}, u \le \frac{v}{4y}A^{\frac{2}{1-B}} \tag{18}$$

$$\frac{\tau_w}{\rho} = \left(\frac{1-B}{2}A^{\frac{1+B}{1-B}}\left(\frac{v}{y}\right)^{1+B} + \frac{1+B}{A}\left(\frac{v}{y}\right)^{B}|u|\right)^{\frac{1}{1+B}}, \quad u > \frac{v}{4y}A^{\frac{2}{1-B}} \tag{19}$$

The proposed law of the all has been widely used in practical computations due to its ability to avoid iterative procedures to compute friction velocity and wall shear stress.However, the proposed law of the wall has several drawbacks. The first drawback is that it does not include the effect of pressure gradients. The second drawback is that the piece-wise expression does not lead to a smooth transition from the laminar sublayer to the inertial region in the buffer zone. Finally, the proposed law of the wall is not accurate for very large values of y_τ^+. Therefore, despite its simplicity and computational efficiency, Werner and Wengle's law of the wall should only be used in specific applications to avoid errors.

Similarly, wall functions proposed by von Karman [27], Deissler[28], Rannie [29], and Reichardt [30] suffer from the same problem of not including the pressure gradient in its formulation and needing the Newton iterations to evaluate the wall-shear stress.

Alternative approaches to defining the explicit law of the wall include direct integration of boundary layer equations [31] and transported turbulence quantities to obtain the friction velocity. For example, if k–ε turbulence models [7, 32-34] are used in simulations, it is possible to employ the following expression to compute the friction velocity directly from the transported quantities:

$$u_t = C_\mu^{\frac{1}{4}} k^{\frac{1}{2}}, C_\mu = 0.09 \tag{20}$$

Equation 20 applies only to models that evaluate turbulent kinetic energy. In addition, the turbulent kinetic energy requires a wall function that sets the correct behavior near the wall. The wall function for k as a function of y_t^+ must be carefully chosen to obtain the correct scaling of turbulent viscosity in the near-wall region, i.e., $v_t^+ \sim \left(y_t^+\right)^3$.The absence of pressure gra–dient in the definition of the wall function for turbulent kinetic energy makes this approach unsuitable for non-equilibrium boundary layer flows.

The direct integration of Equation 5 was proposed by Kalitzin et al. [31]. The simplified RANS equations for the boundary layer flow were integrated using a numerical method for a range of values of non-dimensional wall distance y_t^+. The computed values of the non-dimensional velocity u^+ were then tabulated to obtain the implicitly defined law of the wall. The implicit nature of the tabulated solution is due to the mutual dependence of non-dimensional wall distance and the velocity on the friction velocity. Kalitzin et al. proposed to define a new variable

$$r^+ = u^+ y_t^+ \tag{21}$$

The proposed variable avoids the implicit nature of the tabulated solution as it eliminates the friction velocity from its expression. Therefore, the non-dimen–sional velocity was tabulated against the new variable as this approach allowed direct evaluations of the wall-shear stress. Using tables to obtain the solution for the velocity u^+ avoids the need for the numerical solution of the simplified RANS equation. However, an interpolation procedure is required to evaluate the table values for any intermediate values of r^+ that were not precom–puted. The interpolation proce–dure inevitably introduces the error due to interpolation that can be reduced if the solution is obtained on a larger number of integration points. The main advantage of the tabulated method is using the new variable to avoid Newton iterations. However, the drawback of the method is that the resulting table did not depend on the pressure gradients making the approach unsuitable for non-equili–brium boundary layer flows. Despite its drawbacks, the use of the new variable paved the way for redefining the wall of the law into its explicit form proposed in this work.

2.2 Non-zero-pressure gradient wall functions

The inclusion of pressure gradients in the formulation of wall functions is of great importance for practical flow simulations. Therefore, wall functions that include pres–sure gradients in their formulation are commonly known as generalized or non-equilibrium wall functions.

Such wall functions and other attempts to incor–porate pressure gradients into the law of the wall are described extensively in the literature [20, 23, 35-42]. Kim and Choudhury [20] relied on the two-layer approach described by Launder [33]. They created an expression that includes a logarithmic velocity function of the kinetic energy. A description of shear stress based on this expression necessitates information about the turbulent kinetic energy within the boundary layer. A more generalized form of the wall function in [20] is presented in Equation 22, which does not require turbulent kinetic energy transport computation.

$$C_U^+ \tag{22}$$

where p^+ is defined as follows

$$p^+ = \frac{v}{\rho u_t^3}\frac{dp}{dx} \tag{23}$$

Equation 22 still requires an iterative procedure to calculate wall shear stress and is implicitly defined. In addition, the expression is inconsistent withthe expe–riment for large values of y_t^+ in larger pressure gra–dients. A non-equilibrium wall function proposed by Röber [22] combines the analytical expression for the viscous sublayer with a van Driest damping function. However, similarly to that proposed by Kim and Choudhury, the wall function is limited in utility to smaller values of y_t^+ and still requires an implicit pro–cedure for evaluation. Other attempts to improve the accuracy of these wall functions come in the form of three-zonal wall functions, such as that proposed by Chmielewski and Gieras [43], which is more accurate in modeling the mean streamwise velocity profile. How–ever, because it still models the inner and outermost portions of the boundary layer in the same manner as more two-zonal wall functions, it faces many of the same limitations.

A slightly different approach to non-equilibrium wall functions comes from Duprat *et al.* [44], which relies on velocity scaling and van Driest damping. This combination allows for a continuous wall function [45]. Despite this utility, it is still an implicit method and requires an iterative procedure for friction velocity. In addition, it is similar to those methods proposed by Kim, Choudhury, and Röber, as it deviates from experiments for large wall distance values.

A non-equilibrium wall function that includes acceleration terms was developed by Popovac and Hanjalić [21]. The wall function is described in Equations 24-26 where $E = e^{B\kappa}$ and C_U^+ and a simplified form is shown in Equation 27.

$$u^+ = \frac{1}{\kappa\psi}\ln Ey_t^+ \tag{24}$$

$$\psi = 1 - \frac{C_U^+ y_t^+}{u^+\kappa} \tag{25}$$

$$C_U^+ = \frac{v}{\left(\rho u_t^3\right)}\left[\rho\frac{\partial u}{\partial t} + \rho u\frac{\partial u}{\partial x} + \rho v\frac{\partial u}{\partial y} + \frac{\partial p}{\partial x}\right] \tag{26}$$

$$f_2\left(y_p^+\right) = \begin{cases} 0.5\left(y_p^+\right)^2 - 7.31\times10^{-3}\left(y_p^+\right)^3 \ if \ y_p^+ \le 4 \\ -15.138 + 8.4688y_h^+ - 0.81976\left(y_p^+\right)^2 \\ +3.7292\times10^{-2}\left(y_p^+\right)^3 - 6.3866\times10^{-4}\left(y_p^+\right)^4 \\ if \ 4 \le y_p^+ \le 15 \\ 11.925 + 0.934y_p^+ - 2.7805\times10^{-2}\left(y_p^+\right)^2 \\ +4.6262\times10^{-4}\left(y_p^+\right)^3 \ if \ 15 \le y_p^+ \le 30 \\ 5\ln\left(y_p^+\right) + 8 if \ 30 \le p_p^+ \end{cases} \tag{27}$$

The above-generalized wall function is accurate in various flow regimes, including recirculation zones [46, 47], but requires an iterative calculation of wall shear stress. Additionally, the wall function will compute negative values of velocity at large y_t^+ in environments with large adverse pressure gradients. In environments with large favorable pressure gradients, the generalized expression will diverge from experimental data and overestimate velocity values. As with all other non-equilibrium wall functions discussed so far, it is unbounded for large y_t^+.

One wall function that is not unbounded for large y_t^+ was proposed by Shih *et al.* [23]. The model uses a velocity scale that incorporates the effects of both viscosity and gradients of pressure. The model also blended the buffer region to ensure a continuous wall function across all values of y_t^+. The model proposed by Shih was based on work done by Lumley [13] and shows excellent agreement with the experiment for a wide range of pressure gradients and y_t^+ values. How-ever, the model is limited in its applications due to its complex implementation. The model itself is also implicit. While several works have improved upon the model proposed by Shih, including that by González *et al.* [48] and Hickel *et al.* [49], these works also contain similar complexity in implementation and the need for an iterative procedure.

Except for the Werner and Wengle formulation [19, 26], all wall functions proposed in the literature require an iterative procedure to calculate wall shear stress. The Werner and Wengle formulation is not applicable for flows with a pressure gradient. So a new wall function must be developed to have a globally applicable model that does not require an iterative procedure. In previous works, attempts to do this were limited by the use of y_t^+ and u^+, which are both functions of friction velocity u_t. Thus, a novel transformation of variables is required to circumvent the need for an iterative procedure. This transformation of variables allows for converting the generalized Shih *et al.* model into an explicit for–mulation. The Shih *et al.* model was chosen as it agrees with the experiment for a broad range of wall distance values and incorporates pressure gradient effects.

3. TRANSFORMATION OF VARIABLES

Kalitzin et al. indicated that using the new variable defined as a product of the non-dimensional velocity and wall-distance given by Equation 28 removes the need for the iterative procedure to compute the friction velocity. The proposal of Kalitzin defines an approach to formulating wall functions that satisfy the requi–rement for non-iterative evaluation of wall shear stress. The non-iterative evaluation of the wall shear stress was one of the present work's goals stated in the introduction section. However, the relationship defined by Equation 28 is not a simple convenience expression. Therefore, to see the meaning of the new variable, the new local velocity scale is introduced as follows:

$$\hat{u} = \frac{v}{y} \tag{28}$$

The proposed form of the velocity scale is obtained from the dimensional arguments, and it is used to define a normalized time-averaged velocity denoted by the symbol r^+ as follows:

$$r^+ = \frac{u}{\hat{u}} \tag{29}$$

Therefore, the new variable represents the normalized velocity in the boundary layer related to non-dimensional velocity and wall-distance through Equation 28.

The newly defined variable was used in this work to define a variable transformation to define the law of the wall in an analytical instead of a tabulated form suitable for the non-iterative evaluation of the wall-shear stress. Starting from the incompressible boundary layer equation

$$\left(1+v_t\right)\frac{du^+}{dy_t^+} = 1 + p^+ y_t^+ \tag{30}$$

where

$$\begin{aligned} &u^+ = \frac{u_1}{u_t}, y_t^+ = \frac{u_t y}{v}, v_t^+ = \frac{v_t}{v}, \\ &p^+ = \frac{v}{\rho u_t^3}\frac{dp}{dx}, u_t^2 = \frac{|\tau_w|}{\rho} \end{aligned} \tag{31}$$

the new form of the incompressible boundary layer equation in new variables is obtained as follows:

$$\left(1+\eta_t^+\right)du^+ = dr^+ + p^+ r^+ dy_t^+ \tag{32}$$

Here η_t^+ is the transformed normalized turbulent viscosity defined as

$$\eta_t^+ = u^+\left(1+v_t^+\right) + y_t^+ - 1 \tag{33}$$

Equations 30 and 32 are equivalent and can be transformed into each other with the help of the differential identity

$$d\left(r^+\right) = d\left(u^+ y_t^+\right) = y_t^+ du^+ + u^+ dy_t^+ \tag{34}$$

Equation 32 represents the differential equation in a new set of variables. To get the law of the wall in the new set of variables, Equation 32 has to be integrated. The transformedlaw of the wall in new wall units is equivalent to the law in traditional wall units. The equivalence was demonstrated in **Appendix A** and **B** for Prandtl's and Musker's hypotheses.

4. GENERALIZED WALL FUNCTION FORMULATION IN NEW VARIABLES

Generalized wall functions were proposed by Shih *et al.* [23, 35] to include pressure gradients in the law of the wall. The proposal by Shih is taken in this work to satisfy the second requirement that wall functions must apply to equilibrium and non-equilibrium boundary layer flows. The main idea of generalized wall functions was to introduce a new velocity scale that describes both viscous and pressure effects. The symbol u_c denoted the new velocity scale, and it is used to scale the linearized streamwise RANS equation as follows:

$$v\frac{\partial u}{\partial y} - \overline{u'v'} = \frac{\tau_w}{\rho} + \frac{y}{\rho}\frac{dp_w}{dx} \tag{44}$$

and obtain the generalized solution of the law of the wall with pressure gradients effects [23]

$$\frac{u}{u_c} = \frac{\tau_w}{\rho u_t^2}\frac{u_t}{u_c} f_1\left(y_C^+ \frac{u_t}{u_c}\right) + \frac{\frac{dp}{dx}}{\left|\frac{dp}{dx}\right|}\frac{u_p}{u_c} f_2\left(y_C^+ \frac{u_p}{u_c}\right) \tag{45}$$

where the new velocity scale was defined as

$$u_c = u_t + u_p \tag{46}$$

where u_c is the new velocity scale, u_t is the friction velocity, and u_p is the pressure gradient velocity. Friction velocity was defined using the familiar expression

$$u_t = \sqrt{\frac{|\tau_w|}{\rho}} \tag{47}$$

And the pressure gradient velocity was defined by the following expression

$$u_p = \left(\frac{v}{\rho}\left|\frac{dp_w}{dx}\right|\right)^{\frac{1}{3}} \tag{48}$$

The new velocity scale gives rise to the new definition of the non-dimensional wall-distance variable

$$y_c^+ = \frac{u_c y}{v} \tag{49}$$

The new non-dimensional wall-distance variable is more general as it includes both friction and pressure effects in its definition. The new non-dimensional wall-distance definition is in sharp contrast to the classical non-dimensional wall-distance variable that neglects any pressure effects.

The general solution in Equation 44 consists of two linearly additive parts. The linearly additive nature of the solution allows forthe separation of Equation 44 into two components [13, 23]:

$$v\frac{\partial u_1}{\partial y} - \left(\overline{u'v'}\right)_1 = \frac{\tau_w}{\rho} \tag{50}$$

$$v\frac{\partial u_2}{\partial y} - \left(\overline{u'v'}\right)_2 = \frac{y}{\rho}\frac{dp_w}{dy} \tag{51}$$

The corresponding solutions of Equations 50 and 51 read

$$\frac{u_1}{u_r} = \frac{\tau_w}{\rho u_t^2} f_1\left(y_t^+\right) \tag{52}$$

$$\frac{u_2}{u_p}=\frac{v}{\rho}\frac{\left(\frac{dp_w}{dx}\right)}{u_p^3}f_2\left(y_p^+\right) \tag{53}$$

Equations 51 and 53 give rise to a new normalized wall distance

$$y_p^+=\frac{u_p y}{v} \tag{54}$$

accounting for pressure effects.

The ability to separate Equation 44 into two com–ponent equations accounting for friction and pressure effects results from introducing the new velocity scale and the linearization of the initially non-linear momen–tum equation. One significant advantage of the for–malism used in Shih *et al.* is the complete separation of friction and pressure effects, allowing for their separate treatment. Therefore, in principle, it is possible to vali–date any hypothesis for the friction part independently of the pressure part of the solution. Such property allows for great flexibility and allows, for example, the use of Musker's hypothesis in a generalized wall function.

The law of the wall given by Equation 45 was defined in terms of the new velocity scale u_c, which is difficult to use directly. Therefore, the reformulation of the generalized wall function was proposed in this work to simplify the evaluation of the friction velocity. The new function sgn(*arg*), defined as having a value of+1 if *arg* > 0 and -1 if *arg* < 0, was introduced in Equation 45 to simplify the notation

$$\frac{u}{u_c}=\mathrm{sgn}\left(\tau_w\right)\frac{u_r}{u_c}f_1\left(y_t^+\right)+\mathrm{sgn}\left(\frac{dp_w}{dx}\right)\frac{u_p}{u_c}f_2\left(y_p^+\right) \tag{55}$$

Regrouping the terms in Equation 55 and solving for the friction velocity yields the following definition of friction velocity

$$u_t=\frac{\left(u-u_p\right)\mathrm{sgn}\left(\frac{dp_w}{dx}\right)f_2\left(y_p^+\right)}{\mathrm{sgn}\left(u_1\right)f_1\left(y_t^+\right)} \tag{56}$$

Additional manipulations of Equation 56 provide a simplified expression for the friction velocity:

$$u_t=\frac{\left(u-u_p\right)\mathrm{sgn}\left(\frac{dp_w}{dx}\right)f_2\left(y_p^+\right)}{\mathrm{sgn}\left(u_1\right)f_1\left(y_t^+\right)} \tag{57}$$

Equation 57 is a new form of friction velocity that is very convenient for evaluating the friction velocity. Ho–wever, it should be noted that Equation 57 is still an implicit function, and Newton iterations are required to evaluate it.

In Shih *et al.* [23, 35], the solution to the friction part of the law of the wall given by Equation 57 was based on the experimental observation, and the corres–ponding curve fit as follows:

$$f_1\left(y_t^+\right)=\begin{cases}y_t^+ +0.01\left(y_t^+\right)^2-2.9\times10^{-3}\left(y_t^+\right)^3\\ if\ y_t^+\le 5\\ -0.872+1.465y_t^+-0.0702\left(y_t^+\right)^2+0.00166\left(y_t^+\right)^3\\ -1.495\times10^{-5}\left(y_t^+\right)^4\\ if\ 5\le y_t^+\le 30\\ 8.6+0.1864y_t^+-0.002\left(y_t^+\right)^2+1.144\times10^{-5}\left(y_t^+\right)^3-\\ -2.551\times10^{-8}\left(y_t^+\right)^4\\ if\ 30\le y_t^+\le 140\\ 2.439\ln\left(y_t^+\right)+5 \qquad if\ 140\le y_t^+\end{cases} \tag{58}$$

The pressure part of the law of the wall was defined to be

$$f_2\left(y_p^+\right)=\begin{cases}0.5\left(y_p^+\right)^2-7.31\times10^{-3}\left(y_p^+\right)^3\ if\ \ y_p^+\le 4\\ -15.138+8.4688y_h^+-0.81976\left(y_p^+\right)^2\\ +3.7292\times10^{-2}\left(y_p^+\right)^3-6.3866\times10^{-4}\left(y_p^+\right)^4\\ if\ 4\le y_p^+\le 15\\ 11.925+0.934y_p^+-2.7805\times10^{-2}\left(y_p^+\right)^2\\ +4.6262\times10^{-4}\left(y_p^+\right)^3\ \ if\ 15\le y_p^+\le 30\\ 5\ln\left(y_p^+\right)+8\,if\ 30\le p_p^+\end{cases} \tag{59}$$

Since the friction part of Equation 57 given by Equation 58 depends on the friction velocity, it has to be transformed into a new set of coordinates to allow an explicit evaluation of the friction velocity. Therefore, a transformed function $g_1(r+)$ was introduced into Equa–tion 57 to make it explicit:

$$g_1\left(r^+\right)=\begin{cases}\sqrt{r^+}\ if\ 0\le r^+<24.44\\ 2.8957\ln\left(r^+\right)-4.4958 \quad if\ 24.44\le r^+<378.3\\ 2.3513\ln\left(r^+\right)-1.2777 \quad if\ 378.3\le r^+<2275\\ 2.1973\ln\left(r^+\right)-0.0873 \quad otherwise\end{cases} \tag{60}$$

With the help of the function $g_1(r^+)$, the explicit expression for the wall-shear stress was defined as

$$\tau_w = \rho \left(\frac{\left(u - u_p \operatorname{sgn}\left(\frac{dp_w}{dx} \right) f_2\left(y_p^+ \right) \right)}{\operatorname{sgn}\left(u_1 \right) g_1\left(r^+ \right)} \right)^2 \quad (61)$$

Equation 61 enables the wall-shear stress evaluation in a new wall unit r^+ that is independent of friction velocity. Therefore, the proposed form of wall-shear stress is very convenient for implementation in CFD codes. It requires exactly one function evaluation without iterations to calculate the value of the local wall-shear stress on finite volume face at the wall boundary. Equation 61 was previously unknown and represented the significant finding proposed in this work.

5. ILLUSTRATIVE EXAMPLES OF WALL FUNCTIONS IN TRANSFORMED VARIABLES

A demonstration of the usefulness of the findings in this work is necessary to show its applicability to relevant problems. To illustrate this, numerous examples were compiled, each of which was solved using the generalized wall functions in the new set of proposed variables. In the examples described in the following sections, the k-ω SST model [21] was used to calculate the turbulent viscosity field, μ_t. The governing equations used in the k-ω SST model are described in equations D1-D3 in Appendix D. Boundary conditions far from the way were prescribed as in [21]. Boundary conditions near the solid wall were defined based on the asymptotic near-wall behavior of transport equations for both k and ω [31]. The definition of boundary conditions allowed for a well-posed problem with a specified no-slip condition at the wall.

The following sections focus on computations that are not wall-resolved, meaning that the mesh cell immediately adjacent to the wall produces a y^+ value greater than 1. Equation 61 was used to determine wall shear stress for the meshes, and k and ω fields near the wall were specified according to equations D1-D6 in Appendix D.

The two studies demonstrating the new non-equilibrium wall functions were flow over a backward-facing step [50] and a diffuser [51]. Both are examples of flow with an adverse pressure gradient and separation for which there are quality experimental measurements. They are thus ideal for validating applications of the wall function boundary conditions as defined in Equations 61, D4, and D5.

Caelus, a second-order finite volume solver library, was used in all computational studies [52, 53]. A second-order upwind discretization methodology was used for the convective terms of the momentum and turbulence equations, while a central discretization scheme was used for the diffusive fluxes [54]. Four meshes with various grid resolutions were created by successive uniform mesh refinement. Uniform mesh refinement was used to maintain a constant aspect ratio for all cells across the four meshes while allowing for varying values of y_τ^+. The computational setup allowed for a parametric evaluation of the proposed general wall functions. A k - ω SST transport model [55] was used in each computation, but the proposed wall functions are not limited to one turbulence model. They can be applied to other equilibrium and non-equilibrium turbulence models.

5.1 Backward-facing step study

Driver and Seegmiller collected extensive experimental data on flow over a backward-facing step, including information about various top wall deflections [50]. Changing the top wall deflection angle affected the pressure gradient of the step, which in turn impacted the reattachment point of the flow. The computation in this work focused on a zero-angle deflection of the top wall. Results from the calculation were compared with reattachment point measurements, pressure and friction coefficients along the top and bottom walls, and velocity profile measurements provided by Driver and Seegmiller.

The mesh used in the computation consisted of a hexahedral mesh 40h upstream and 50h downstream of the step, where h is the height of the step. The dimensions were chosen to ensure that the flow was not influenced by boundary conditions. The mesh height was 8h upstream of the step and 9h downstream. A magnified section of the 65,000 cell mesh, centred on the backward-facing step, is shown in Figure 1, along with relative domain dimensions.

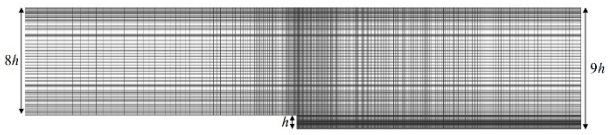

Figure 1. Detail of Backward-facing step mesh. All spatial dimensions were normalized by the step height, *h*.

Atmospheric pressure and temperature were used for inlet boundary conditions. The inlet velocity was 44.2*m/s,* and the turbulence intensity value was 0.061%. The number of elements, as well as the y_τ^+ value at the wall for each mesh, is shown in Table 1.

Table 1. Mesh size (*N*), wall spacing (y_t^+), and aspect ratio (*AR*) are used in mesh refinement study simulations. The mesh aspect ratio (*AR*) was held constantan the refinement process.

Grid Refinement Level		
1	16,000	30
2	65,000	15
3	261,000	6
4	1,046,000	3

The following figures compare experimental and computational results for the various grid refinement levels. Figure 2 shows the computed and experimental friction coefficients at the lower wall for a normalized axial distance ranging from x/h = -5 to x/h = 35. The largest error occurs for the mesh with y_τ^+ = 30 and steadily decreases with mesh refinement. Despite the improvement, all meshes underpredict the friction coefficient for $0 \leq x/h \leq 5$. However, the shapes of the computed and experimental curves are in good agreement for all meshes.

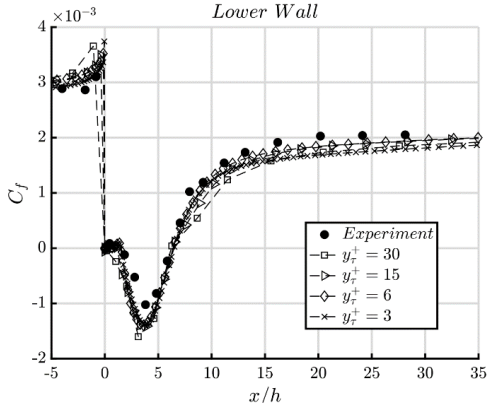

Figure 2. The friction coefficient (C_f) over the lower wall(x/h = -5 to 35) comparison to experiments. Solid circles are experimental measurements of Driver and Seegmiller [50]. Lines represent simulation results with symbols: square – y_t^+ = 30, triangle – y_t^+ = 15, diamond – y_t^+ = 6, and x – y_t^+ = 3.

Figure 3 shows a comparison between computed and experimental lower wall pressure coefficients. As with the friction coefficients, the shapes of the computed and experimental pressure coefficients are in good agreement.

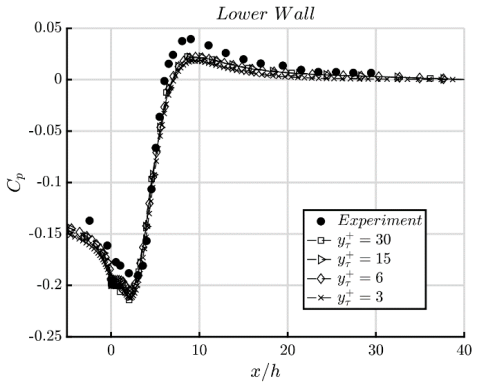

Figure 3. Comparison ofpressure coefficient (C_p) and expe–rimental values.Filled circles [50] and simulated – square – y_t^+ = 30, triangle – y_t^+ = 15, diamond – y_t^+ = 6, and x – y_t^+ = 3.

Figures 4 to 7 show comparisons of the experi–mental and simulated velocity profiles at various nor–malized axial distances. As shown, simulated results agree well with experimental data for x/h = -4, x/h = 1 and x/h = 4. The mesh with y_t^+ = 30 differs from the other mesh results and experimental data for predictions of the location of zero velocity but is otherwise consistent. Differences between computations and experiments grow in magnitude at locations of x/h = 6 and larger.

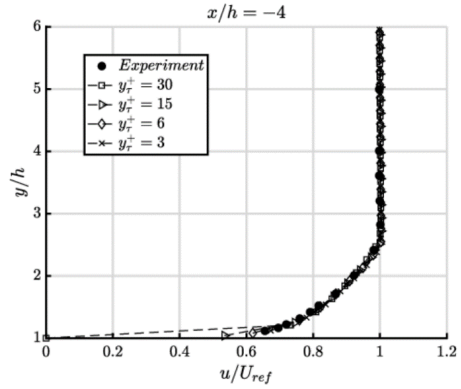

Figure 4. Streamwise velocity distributions at the location x/h = -4 as the function of normalized wall distance, y. The velocity was normalized by the reference velocity, U_{ref}, defined in Reference [50] for each simulation.

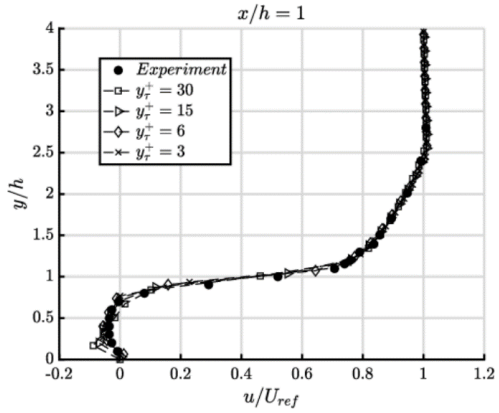

Figure 5. Streamwise velocity distributions at the location x/h = 1 as the function of normalized wall distance, y,. The velocity was normalized by the reference velocity, U_{ref}, defined in Reference [50] for each simulation.

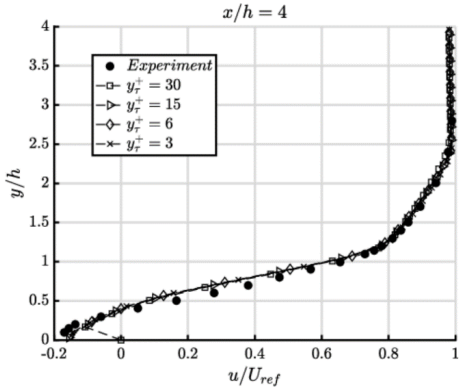

Figure 6. Streamwise velocity distributions at the location x/h = 4 as the function of normalized wall distance, y,. The velocity was normalized by the reference velocity, U_{ref}, defined in Reference [50] for each simulation.

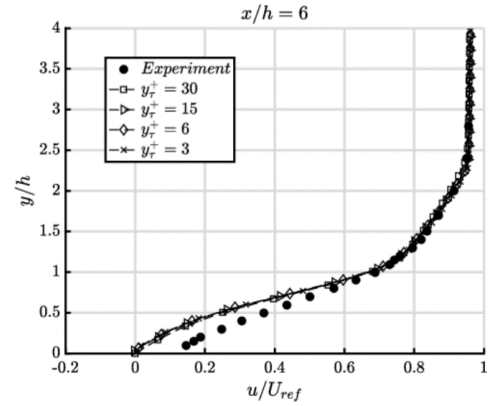

Figure 7. Streamwise velocity distributions at the location x/h = 6 as the function of normalized wall distance, y,. The velocity was normalized by the reference velocity, U_{ref}, defined in Reference [50] for each simulation.

5.2 Asymmetric Plane Diffuser Study

Experimental data for asymmetric flow in a plane diffuser [56] was collected by Obi and Matsuda [51]. The experiment analyzed fully turbulent flow, which causes separation and flow reattachment at the lower wall of the diffuser. The complex nature of the flow field makes simulating the turbulence behavior challenging for many models. In addition, separation regions also pose quality challenges for evaluating and testing wall functions.

The mesh used in the computation consisted of a hexahedral mesh. All dimensions were normalized by the channel height, h. The expansion ratio of the diffuser is 4.7, and the flow inlet is 110h upstream. The outlet is 55h downstream of the plane diffuser. Figure 8 shows the 20,000 element mesh with relevant domain dimensions.

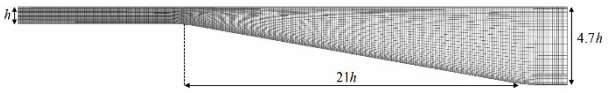

Figure 8. Computational mesh for the plane diffuser with 20,000 cella.

The boundary conditions used in the simulation were identical to those used in [51]. The inlet velocity was u = 0.3 m/s and the turbulent kinetic energy and specific dissipation rate were as k = 0.2945755 m^2/s^2 and ω = 97.37245 1/s, respectively. The walls were modelled using the no-slip conditions, and the zero Neumann condition was applied to the flow outlet.

The computation was run on four different meshes, beginning with a coarse mesh that underwent successive uniform grid refinement to produce the other three meshes. The refinement was performed to ensure that the cell aspect ratio remained constant for all meshes. The four meshes, along with the number of elements and y_t^+ for each, is shown in Table 2.

Table 2. Mesh size (*N*), wall spacing (y_t^+), and aspect ratio (*AR*) were used for the plane diffuser simulations.The mesh aspect ratio (*AR*) was held constantan the refinement process.

Grid Refinement Level	N	y_t^+
1	5,000	40
2	20,000	20
3	82,000	10
4	332,000	5

The distribution of y_t^+ at the bottom wall for each mesh is shown in Figure 9. Figure 10 and Figure 11 show comparisons between experimental and compu–tational data for both pressure coefficients at the bottom wall and velocity profiles within the diffuser. As shown, the shapes of all computed curves are in good agreement with that of the experiment, with the largest error present in the $y_t^+ = 40$ case.

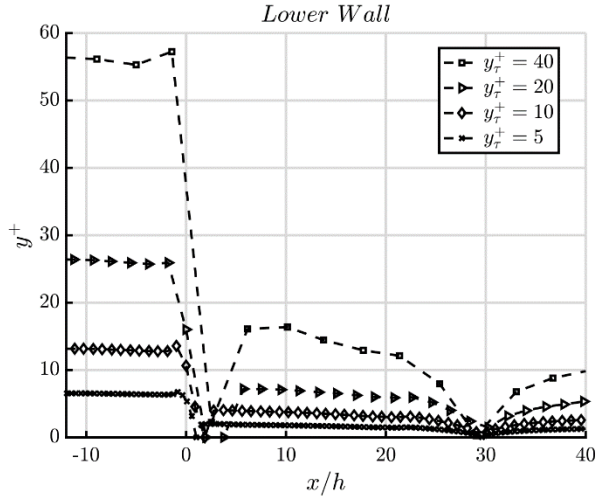

Figure 9. Lower wall y_t^+ variations for each grid resolution.

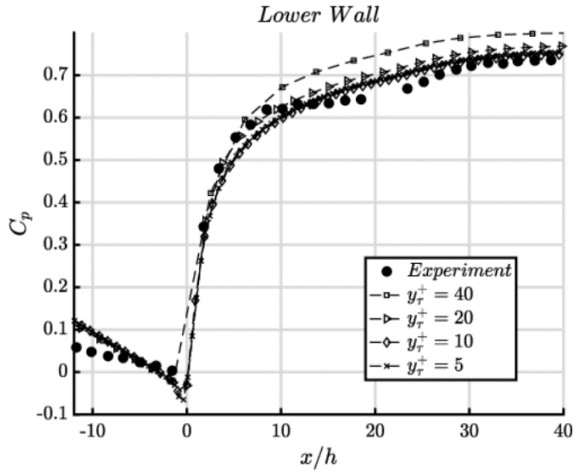

Figure 10. Plane diffuser lower wall distribution of coeffi–cient of pressure.

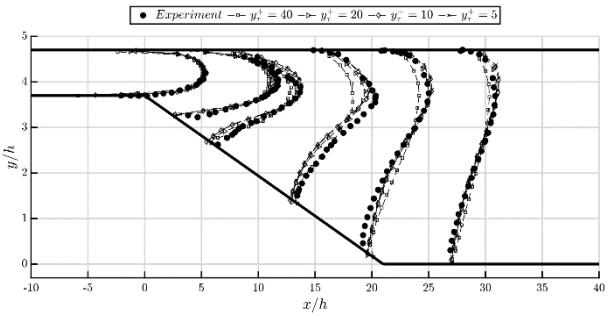

Figure 11. Normalized streamwise velocity profiles at *x/h* = -5.8, *x/h* = *2.6*, *x/h* = 6, *x/h* = 13.5, *x/h* = 20 and *x/h* = 27.

6. SUMMARY AND CONCLUSIONS

A novel non-iterative formulation of wall functions that applies to equilibrium and non-equilibrium boundary layer flows was proposed. The proposed formulation uses a set of variables that are more useful for computational codes as they allow for calculating wall shear stress without an iterative procedure. An explicit form of the formulation is provided for laws of the wall that do and do not include the effects of pressure gradients. A new near-wall variable r^+ was created by normalizing the local velocity, which allowed for an explicit definition of the wall shear stress. The new formulation was validated in two key ways. The first was by demonstrating that applying the new variables to the existing law of the wall formulations yielded the same established wall shear stress values. The second validation was through a computational study of a backward-facing step and a plane diffuser. Both computational studies demonstrated the new formulation's effectiveness in handling pressure gradient effects. In addition, the computational studies have shown that the new formulation converged to measured experimental results with sufficient mesh refinement.

APPENDIX A: PRANDTL'S LAW OF THE WALL IN NEW VARIABLES

The differential equation for the boundary layer flow in the case of zero-pressure gradient flow is defined to be

$$\left(1+v_t^+\right)du^+ = dy_t^+,\ p=0 \qquad \text{(A1)}$$

Prandtl's hypothesis stated that in the laminar sub–layer, the turbulent viscosity is negligible, i.e.

$$v_t^+ \ll 1 \tag{A2}$$

Substitution of Equation A2 into Equation A1 yields the following expression for the laminar sublayer

$$du^+ = dy_t^+ \tag{A3}$$

The solution of Equation A3 defines the law of the wall for the laminar sublayer portion of the boundary layer under Prandtl's hypothesis:

$$u^+ = y_t^+, y_t^+ < 5 \tag{A4}$$

Equivalently, the transformed viscosity under the same assumptions becomes

$$\eta_t^+ = u^+ + y_t^+ - 1 \tag{A5}$$

The differential equation of the laminar sublayer is defined to be

$$\left(u^+ + y_t^+\right) du^+ = dr^+ \tag{A6}$$

Using Equation A4, the differential equation was integrated to read

$$u^+ = \sqrt{r^+}, r^+ \le 5^2 \tag{A7}$$

Equation A7 defines the law of the wall for the laminar sublayer in terms of new variables.

Prandtl's hypothesis postulates that the normalized turbulent viscosity is much greater than unity in the inertial region of the boundary layer

$$v_t^+ \gg 1 \tag{A8}$$

therefore, the normalized transformed turbulent visco–sity becomes

$$\eta_t^+ = u^+ v_t^+ + y_t^+ - 1 \tag{A9}$$

Using the normalized transformed viscosity expre–ssion in the transformed RANS equation of boundary layer flow yields the following expression:

$$\left(u^+ v_t^+ + y_t^+\right) du^+ = dr^+ \tag{A10}$$

Prandtl's hypothesis for the inertial region in new variables takes the new form

$$v_t^+ = \frac{k_t r^+ - y_t^+}{u^+} \tag{A11}$$

where k_t was defined to be

$$k_t = \kappa + \frac{1}{u^+} \tag{A12}$$

The solution of Equation A10 is

$$u^+ = \frac{1}{\kappa} \ln\left(r^+\right) + C, \; r^+ \ge 10.8^2 \tag{A13}$$

The contribution of the normalized velocity to k_t is negligible for large r^+ values. The function k_t is appro–ximated by a constant value obtained from the curve fit

$$k_t = \frac{1}{2.1108}, \; C = 0.7576 \tag{A14}$$

The Comparison between the law of the wall in wall units and transformed variables is shown in Figure A1. The agreement between the two curves is excellent. Therefore, it is possible to use new variables to obtain the classical results under the same hypothesis. However, the significant advantage of the newly defined law of the wall is that the Newton procedure is not needed to evaluate the wall shear stress directly. It should be noted that the laminar sublayer region was extended through the buffer zone for convenience.

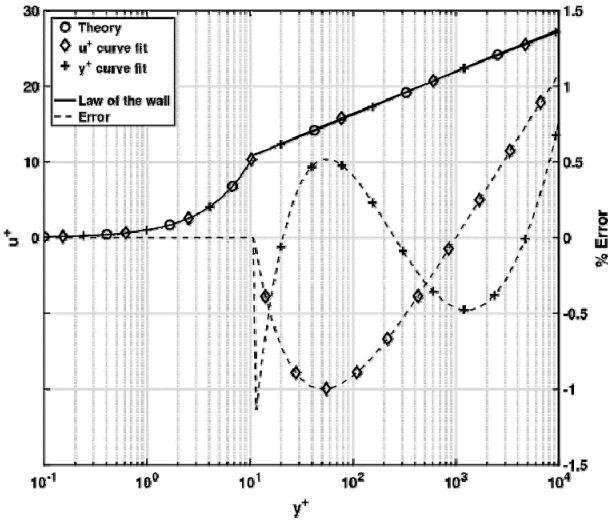

Figure A1. Comparison of the original and transformed wall functions. The solid line labeled $f(y_t^+)$ corresponds to the wall function defined with respect to y_t^+ given by Equation A4 and Equation A7. Dashed line labeled $g(r^+)$ corresponds to the wall function defined as a function of variable r^+ and given by Equation A4 and Equation A7. The viscous sublayer solution was extended to values $y_t^+ \le 10.8$ for comparison purposes. The dashed lines indicate the percent error from the law of the wall.

APPENDIX B: MUSKER'S LAW OF THE WALL IN NEW VARIABLES

Musker's law of the wall was based on the inverse weighting between the logarithmic region and the buffer zone profiles to obtain one continuous representation of the law of the wall valid for all values of non-dimen–sional wall distance. It is possible to apply the same approach used in Prandtl's hypothesis to express the profile in new variables. However, a curve fitexpresses Musker's profile in new variables. Curve fitting is a general approach to expressing the law of the wall cor–responding to any underlying hypothesis in new variables. In general, the curve fit minimizes the error in the least-squares sense. Therefore, all that is needed is the expression of the law of the wall that is used to evaluate the function for various values of the non-dimensional wall distance. In the case of Musker's function, the law of the wall becomes

$$u^+ = \frac{1}{k}\ln\left(\frac{\sqrt{r^+}+a}{a}\right)+\frac{\alpha}{a+4\alpha}\left\{(a-4\alpha)\right.$$
$$\ln\left[\frac{a\left[\left(\sqrt{r^+}-\alpha\right)^2+\beta^2\right]}{2\alpha\left(\sqrt{r^+}+a\right)^2}\right]+\frac{2\alpha(5a-4\alpha)}{\beta} \quad \text{(B1)}$$
$$\left.\left[\tan^{-1}\left(\frac{\sqrt{r^+}-\alpha}{\beta}\right)\right]+\tan^{-1}\left(\frac{\alpha}{\beta}\right)\right]\Bigg\}$$

Various symbols appearing in Equation B1 are defi–ned as follows

$$a = l+\frac{1}{9c^2 l}+\frac{1}{3c} \quad \text{(B2)}$$

$$l = \left(\frac{1}{2}\frac{\sqrt{\frac{4s+27c^3}{27c}}}{cs}+\frac{2s+27c^3}{54c^3 s}\right)^{\frac{1}{3}},\ c = 0.23 \quad \text{(B3)}$$

$$s = 8.347\times10^{-4}$$

$$2\alpha = \alpha-\frac{1}{c},\ \beta^2 = 2a\alpha-\alpha^2$$

Equation B1 does not need any iterations to evaluate the friction velocity since the new form of Musker's function defines an explicit relationship between u^+ and r^+. Therefore, only one evaluation of Equation 50 is required per face of the finite volume lying on the wall boundary.

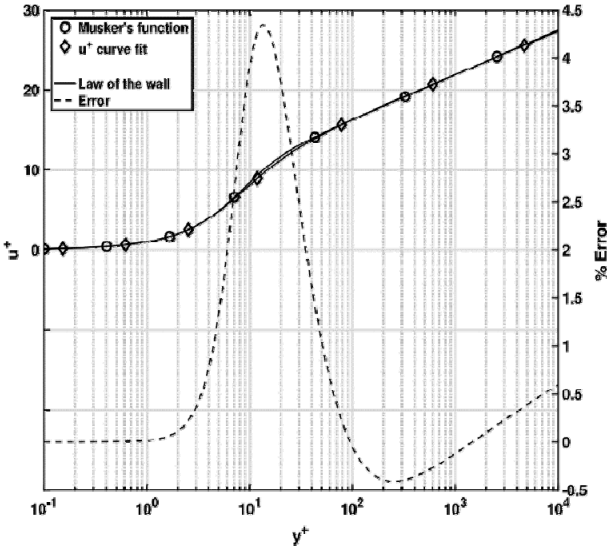

Figure B1.Comparison of the original and transformed wall functions.The solid line with diamonds corresponds to that incompressible boundary layer in new units, Equation B1. The solid line with circles is Musker's function. The dashed lines indicate percent error from Musker's law of the wall.

APPENDIX C: *k - ω* SST TURBULENCE MODEL

Turbulent viscosity field μ_t must be known to close the momentum equation. In this work, the turbulent viscosity field was computed by solving the k - ω SST transport equations [55]. The following expressions give the k - ω SST turbulence model for incompressible flows:

$$\frac{\partial(\rho k)}{\partial t}+\frac{\partial\left(\rho u_j k\right)}{\partial x_j} = P-\beta^*\rho w k+ \quad \text{(C1)}$$
$$+\frac{\partial}{\partial x_i}\left[(\mu+\sigma_k\mu_t)\frac{\partial k}{\partial x_i}\right]$$

$$\frac{\partial(\rho\omega)}{\partial t}+\frac{\partial\left(\rho u_j \omega\right)}{\partial x_j} = \frac{\gamma}{v_t}P-\beta\rho\omega^2+\frac{\partial}{\partial x_j}\Big[(\mu+ \quad \text{(C2)}$$
$$\sigma_\omega\mu_t)\frac{\partial\omega}{\partial x_i}\Big]+2(1-F_1)\frac{\rho\sigma_{\omega2}}{\omega}\frac{\partial k}{\partial x_i}\frac{\partial\omega}{\partial x_i}$$

with the following definitions of terms in Equation C1 and Equation C2:

$$P = \tau_{ij}\frac{\partial u_i}{\partial x_i} \quad \text{(C3)}$$

$$\tau_{ij} = \mu_t 2S_{ij} \quad \text{(C4)}$$

$$\mu_t = \frac{\rho a_1 k}{\max(a,\omega,\Omega F_2)} \quad \text{(C5)}$$

$$F_1 = \tanh\left(\zeta_1^4\right) \quad \text{(C6)}$$

$$v_t^+ \quad \text{(C7)}$$

$$F_2 = \tanh\left(\zeta_2^2\right) \quad \text{(C8)}$$

$$\zeta_2 = \max\left(2\frac{\sqrt{k}}{\beta^*\omega d},\frac{500v}{d^2\omega}\right) \quad \text{(C9)}$$

$$\Omega = \sqrt{2W_{ij}W_{ij}} \quad \text{(C10)}$$

$$W_{ij} = \frac{1}{2}\left(\frac{\partial u_i}{\partial x_i}-\frac{\partial u_j}{\partial x_i}\right) \quad \text{(C11)}$$

Values of constants used in computational studies in this work are as follows:

$$\gamma_1 = \frac{\beta_1}{\beta^*}-\frac{\sigma_{\omega1}\kappa^2}{\sqrt{\beta^*}} \quad \text{(C12)}$$

$$\gamma_2 = \frac{\beta_2}{\beta^*}-\frac{\sigma_{\omega2}\kappa^2}{\sqrt{\beta^*}} \quad \text{(C13)}$$

$$\sigma_{k1} = 0.85,\ \sigma_{\omega1} = 0.5,\ \beta_1 = 0.075,\ \sigma_{k2} = 1.0$$
$$\sigma_{\omega2} = 0.856,\ \beta_2 = 0.0828,\ \beta^* = 0.09$$
$$\kappa = 0.41,\ a_1 = 0.31$$

APPENDIX D: *k - ω* BOUNDARY CONDITIONS

The behaviour of specific dissipation rate and turbulent kinetic energy in the boundary layer was specified as follows:

I. The specific dissipation field ω^+ in the laminar sublayer of the turbulent boundary layer is given by:

$$\omega_{vis}^{+} = \frac{6}{\beta_i}\left(y^{+}\right)^2 \tag{D1}$$

$$\omega^{+} = \frac{\omega v}{u_r^2} \tag{D2}$$

II. The ω^{+} in the logarithmic region of the turbulent boundary value is given by [25]:

$$\omega_{\log}^{+} = \frac{1}{\kappa\sqrt{C_\mu}\, y^{+}},\ C_\mu = 0.09 \tag{D3}$$

III. The intermediate region between the laminar sublayer is given by:

$$\omega^{+} + \sqrt{\left|\omega_{vis}^{+}\right|^2 + \left|\omega_{\log}^{+}\right|^2} \tag{D4}$$

IV. The k^{+} in the boundary layer was defined as

$$k^{+} = v_t^{+}\omega^{+} \tag{D5}$$

$$k^{+} = \frac{k}{u_r^2} \tag{D6}$$

REFERENCES

[1] Rasuo, B.: On Boundary Layer Control in Two-Dimensional Transonic Wind Tunnel Testing, in: IUTAM Symposium on One Hundred Years of Boundary Layer Research, Solid Mechanics and its Applications, Vol. 129, Springer, Dordrecht, 2006, pp. 473-482, doi: 10.1007/978-1-4020-4150-1_46

[2] Mirkov, N., Rasuo, B., Kenjeres, S.: On the Improved Finite Volume Procedure for Simulation of Turbulent Flows over Real Complex Terrains, Journal of Computational Physics, Vol. 287, No. 15 pp. 18-45, 2015, doi: 10.1016/j.jcp.2015.02.001

[3] Jazarevic, V., Rasuo, B.: Numerical Calculation of Aerodynamic Noise Generated from an Aircraft in Low Mach Number Flight, in: Boundary and Interior Layers, Computational and Asymptotic Methods - BAIL 2016, Editors: Huang, Zhongyi, Stynes, Martin, Zhang, Zhimin, Series: Lecture Notes in Computational Science and Engineering, Vol. 120, pp. 113-128, 2017. doi: 10.1007/978-3-319-67202-1

[4] Jazarevic, V., Rasuo, B.: Numerical prediction of aerodynamic noise generated from missile for low Mach number flows, TehničkiVjesnik-Technical Gazette, Vol. 24, No.3 pp. 663-670, 2017. doi: 10.17559/TV-20141231143143

[5] Jazarevic, V., Rasuo, B.: Computation of acoustic sources for the landing gear during the take-off and landing, FME Transactions, Vol. 41, No. 3, pp. 180-188, 2013.

[6] Launder, B. E.: On the computation of convective heat transfer in complex turbulent flows. Journal of Heat Transfer, Vol. 110, pp. 1112–1128, 1988.

[7] Wilcox, D. C.: Turbulence Modeling for CFD. DCW Industries, Inc., California, 2 edition, 1994

[8] Spalart, P. R. and Allmaras, S. R.: A One-Equation Turbulence Model for Aerodynamic Flows. AIAA-92-0439, January 1992.

[9] Spalart, P. R., and Allmaras, S. R.: A One-Equation Turbulence Model for Aerodynamic Flows, LaRecherche Aérospatiale, no 1, pp. 5-21, 1994.

[10] Durbin, P. A. and Petterson, B. A.: *Reiff. Statistical Theory and Modeling for Turbulent Flows*. John Wiley and Sons, West Sussex, 1 edition, 2011.

[11] Chapman, D. R.: Computational Aerodynamics Development and Outlook, AIAA Journal, Vol. 17, No. 12, pp. 1293-1313, 1979.

[12] Choi, H. and Moin, P.: 'Grid-point requirements for large eddy simulation: Chapman's estimates revisited, Physics of Fluids, Vol. 24, No. 1, pp. 011702, 2012.

[13] Tennekes, H. and Lumley, J. L.: *A First Course in Turbulence*. The MIT Press, Massachusetts, 15 edition, 1994.

[14] Pope, S.: A more general effective-viscosity hypot–hesis. Journal of Fluid Mechanics, Vol. 72 No. 2, pp. 331-340, 1975.

[15] Prandtl, L: A relationship between heat exchange and fluid resistance (in German). A. Physik, Vol. 11, pp. 1072–1078, 1910.

[16] Meier, G.E.A, Sreenivasan, K.R, Heinemann, H.J. (Editors).: IUTAM Symposium on One Hundred Years of Boundary Layer Research, Solid Mecha–nics and its Applications, Vol. 129, Springer, Dordrecht, 2006, doi: 10.1007/978-1-4020-4150-1

[17] Spalding, S. B.: A single formula for the law of the wall. Journal of Applied Mechanics, Transactions of ASME Series E, Vol. 83 pp.455, 1961.

[18] Musker, A. J.: Explicit expression for the smooth wall velocity distribution in a turbulent boundary layer. AIAA Journal, Vol. 17 No. 6, pp. 655–657, 1978.

[19] Werner, H. and Wengle, H.: Large eddy simulation of turbulent flow over and around a cube in a plane channel. Springer-Verlag, Munich, turbulent shear flows 8 edition, 1993.

[20] Kim, S. E., and Choudhury, D: A near-wall treat–ment using wall functions sensitized to pressure gradient. In Separated and Complex Flows. ASME, 1995.

[21] Popovac, M. and Hanjalic, K.: Compound wall treatment for rans computation of complex turbulent flows and heat transfer. Flow Turbulence Combust, Vol. 78, pp. 177–202, 2007.

[22] Dillman, A. editor. Continuous Formulation of Wall Function with Pressure Gradient, pages 411–418. *New Results in Numerical and Experimental Fluid Mechanics*. Springer - Verlag, Berlin Heidelberg, 2013.

[23] Shih, T. H., Povinelli, L. A., Liu, N. S., Potapczuk M. G., and Lumely. J. L.: A Generalized Wall Functions. Technical report, NASA, 07 1999.

[24] Ansys Fluent. ANSYS FLUENT 12.0 Theory Guide, 23 Jan. 2009, www.afs.enea.it/project/neptunius/docs/fluent/html/th/main_pre.htm

[25] Pieringer, P., Sanz, W. A Pressure Gradient Sen–sitive Wall Function for the Prediction of Turbulent Flow in Thermal Turbomachinery. Proceedings of the ASME Turbo Expo 2005: Power for Land, Sea, and Air. Volume 6: Turbo Expo 2005, Parts A and B. Reno, Nevada, USA. June 6–9, 2005.

[26] Efros, V: *Large eddy simulation of channel flow using wall functions*. Master's thesis, Göteborg, Sweden, 2006.

[27] Von Karman, T.: The analogy between fluid friction and heat transfer. Trans. ASME, Vol. 61, pp.705–710, 1939.

[28] Deisssler, R. G.: Analysis of turbulent heat transfer, mass transfer, and friction in smooth tubes at high Reynolds and Schmidt numbers. Technical report, NASA, 1954.

[29] Rannie, W. D.: Heat transfer in turbulent shear flow. Journal of the Aeronautical Sciences, Vol. 23 pp.485, 1925.

[30] Reichardt, H. Complete representation of turbulent velocity aversion in smooth pipes (in German). Z. Agnew Math. Mech., Vol. 31, pp. 208–219, 1951.

[31] Kalitzin, G., Medic, G., Iaccarino, G., Durbin, P: Near-wall behavior of rans turbulence models and implications for wall functions. Journal of Compu–tational Physics, Vol. 204, pp. 265–291, 2005.

[32] Jones, W. P. and Launder, B. E.: The prediction of laminarization with a two-equation turbulence model. International Journal of Heat and Mass Transfer, Vol. 15, pp. 301–314, 1972.

[33] Launder, B. E. and Sharma, B. I.: Application of the energy dissipation model of turbulence to the calculation of flow near a spinning disc. Letters in Heat and Mass Transfer, Vol. 1 No. 2, pp.131–138, 1974.

[34] Hanjalic, K., Launder B. E.: *Modeling Turbulence in Engineering and Environment - Second Moment Routes to Closure*, pages 143–156. Cambridge University Press, Cambridge, 2011.

[35] Shih, T. H., Povinelli, L. A., Liu, N. S.: Application of generalized wall function to complex turbulent flows. Journal of Turbulence, Vol. 4, 2011.

[36] Rona, A., Daurea, G. and Monti, M: On the generation of the mean velocity profile for turbulent boundary layers with pressure gradient under equilibrium conditions. Aeronautical Journal, Vol. 116, 2012.

[37] Rodi, W. and Scheurer G.: Scrutinizing the k - ε Turbulence Model Under Adverse Pressure Gradient Conditions, Jour. Fluids Eng., Vol. 108, pp. 174-179, 1986

[38] Subrahmanyam, M., Cantwell, B. and Alonso, J.: A universal velocity profile for turbulent wall flows including adverse pressure gradient boundary layers, J. Fluid Mech. Vol. 933, No. 16, 2022.

[39] Cantwell, B: A universal velocity profile for smooth wall pipe flow, J. Fluid Mech., vol. 878, pp. 834-874, 2019.

[40] Chauhan, K., Nagib, H and Monkewitz, P.: On the Composite Logarithmic Profile in Zero Pressure Gradient Turbulent Boundary Layers, 45th AIAA Aerospace Sciences Meeting and Exhibit, Reno, Nevada, January 8-11, 2007.

[41] Vujičić, M., Crnojević, C.: Calculation of the Tur–bulent Flow in a Plane Diffuser by using the Integral Method. FME Transactions, Vol. 31, 2003.

[42] Banjac, M. and Vasiljević, B.: Development of a new Near-wall Reynolds Stress Turbulence Model for Jet Impingement Heat Transfer Prediction. FME Transactions, Vol. 32, 2004

[43] Chmielewski, M. and Gieras, M: Three-zonal Wall Function for k - ε Turbulence Models, Computa–tional Methods in Science and Technology, Vol. 19, pp. 107-117, 2013.

[44] Duprat, C. Balarac, G., Metais, O., Congedo P. M. and Brugiere. O.: A wall layer model for large eddy simulations of turbulent flows with/out pressure gradient. Physics of Fluids, Vol. 23 No.1, 2011.

[45] Manhart, M., Peller, N., and Brun, C.: Near-wall scaling for turbulent boundary layers with adverse pressure gradient. Theoretical and Computational Fluid Dynamics, Vol. 22 No. 243, 2008.

[46] Nazif, H. and Tabrizi, H.: Applying a non-equi–librium wall function in k–e turbulent modelling of hydrodynamic circulating flow, Applied Mathema–tical Modelling, Vol. 38, pp. 588-598, 2014.

[47] Nazif, H. and Tabrizi, H.: Comparison of Standard Turbulent Wall Function with a Non-Equilibrium Wall Model, International Journal of Fluid Mecha–nics Research, Vol. 38, No. 6, pp 499-508, 2011.

[48] González, D., Adler, M. and Gaitonde, D.: Large-Eddy Simulation of Compressible Flows with an Analytic Non-Equilibrium Wall Model, AIAA SciTech Forum, Kissimmee, Florida, January 8-12, 2018.

[49] Hickel, S., Touber, E., Bodart, J., Larsson, J.: A Parametrized Non-Equilibrium Wall-Modelfor Large Eddy Simulations, Eight International Symposium on Turbulence and Shear Flow Phenomena, Poitiers, France, August 28-30, 2013.

[50] Driver, D. M. and Seegmiller, H. L.: Features of a reattaching turbulent shear layer in divergent channel flow. AIAA Journal, Vol. 23 No. 2, pp:163–171, 1985.

[51] Obi, S. A. and Masuda, S.: Experimental and computational study of turbulent separating flow in an unsymmetric diffuser. In Ninth Symposium on Turbulent Shear Flows, Kyoto, Japan, August 16 - 19, page 305, 1993

[52] Stephens, D. W., Jemcov, A., Sideroff, C.: Veri–fication and validation of the caelus library: Incompressible turbulence models. In Proceeding of the ASME Fluids Engineering Division Summer Meeting, volume 1. ASME, 2017.

[53] Jemcov, A., Stephens, D. W., Sideroff, C.: Verifi–cation and validation of the caelus library: Incom–pressible flow solvers. In Proceeding of the ASME Fluids Engineering Division Summer Meeting, volume 1. ASME, 2017.

[54] Ferziger, J. H., Perić, M.: *Computational Methods on Fluid Dynamics*, chapter 8. Springer-Verlag, Springer-Verlag Berlin Heidelberg, 3 edition, 2002.

[55] Menter, F. R.: Two-equation eddy viscosity turbu–lence models for engineering applications. AIAA Journal, Vol. 32 No. 8, pp:1598–1605, 1994.

[56] Buice, C. U., Eaton, J. K.: Experimental investi–gation of flow through an asymmetric plane diffu–ser. Journal of Fluids Engineering, Vol. 122 pp: 433–435, 2000.

NOMENCLATURE

k	Turbulent kinetic energy
k^+	Normalized turbulent kinetic energy
p_w	Pressure at the wall
p^+	Normalized pressure
r+	Normalized local averaged velocity
u	Stream-wise component of time-averaged velocity
u_C	Velocity scale related to viscous and pressure effects
u_p	Velocity scale related to pressure effects
u_t	Friction velocity
u^+	Non-dimensional velocity
y	Distance in the wall-normal direction
y^+	Non-dimensional wall-normal distance

Greek symbols

η_t^+	Transformed normalized turbulent viscosity
μ_t	Local turbulent viscosity
ν	Molecular kinematic viscosity
ν_t	Turbulent kinematic viscosity
ν_t^+	Non-dimensional turbulent kinematic viscosity
ρ	Fluid density
σ_{ij}	Viscous stress tensor
τ_w	Wall shear stress
ω	Specific dissipation
ω^+	Normalized specific dissipation

ФОРМУЛА НЕИТЕРАТИВНОГ МОДЕЛА ЗИДА ЗА НЕРАВНОТЕЖНЕ ТОКОВЕ ГРАНИЧНОГ СЛОЈА

А. Јемцов, Ј.П. Гонзалес, Ј.П. Марусзевски, Р.Т. Кели

Предложена је нова неитеративна формулација генерализованих функција зида која се примењује на равнотежне и неравнотежне токове граничног слоја. Предложена формулација користи скуп вари–јабли које су корисније за рачунске кодове јер омо–гућавају израчунавање напона на смицање зида без итеративне процедуре. Поред тога, предвиђена је експлицитна форма формулације која се користи за законе зида са и без градијента притиска. Нова трансформација варијабле трансформише функцију зида у нови облик који поједностављује имплемен–тацију и процену напона на смицање зида у рачунарским кодовима.